

Network RTK Getting Ready for GNSS Modernization

Herbert Landau, Xiaoming Chen, Adrian Kipka, and Ulrich Vollath

SURVEYORS AND GEODESISTS pioneered the use of GPS carrier-phase positioning in the early 1980s when only a few Block I test satellites were in orbit. Receiver measurements were recorded simultaneously at project or rover sites and a reference site and, after collection, the data were post-processed back in the office. Postprocessing of differenced carrier phases became a standard high-accuracy positioning technique and is still frequently used today.

However, some high-accuracy positioning and navigation tasks require real-time operations. In the mid-1990s, real-time kinematic (RTK) positioning was developed. In RTK positioning, a receiver at a reference site makes pseudo-range and carrier-phase measurements, which are transmitted over a radio link to one or more rover receivers in the field. A rover receiver combines its measurements with those received over the radio link and, resolving the carrier-phase ambiguities, accurately determines its coordinates.

Because atmospheric and satellite-position errors decorrelate with increasing distance between reference and rover receivers, the ability to perform successful ambiguity resolution decreases with distance as well. This limits the effective distance between reference stations and rovers. To overcome this limitation efficiently, the concept of network RTK was

developed where data from a number of reference stations are used in a filter to determine the measurement errors across the network and then to provide corrections to rovers or to synthesize data for a virtual reference station (VRS) in the vicinity of a particular rover. As the number of stations in a network grows, the more processing is required to generate corrections and VRS data streams. And as more satellite signals are observed by reference and rover receivers, even higher demands are placed on the network RTK filter processing. In this month's column, we look at an innovative filter technique for significantly extending the number of reference stations that can be supported for network RTK positioning under modernized GNSS.

"Innovation" is a regular column that features discussions about recent advances in GPS technology and its applications as well as the fundamentals of GPS positioning. The column is coordinated by Richard Langley of the Department of Geodesy and Geomatics Engineering at the University of New Brunswick, who welcomes your comments and topic ideas. To contact him, see the "Contributing Editors" section on page 10.

After its introduction in the late 1990s, GNSS network real-time kinematic (RTK) technology based on the virtual reference station (VRS) approach became an accepted and proven technology, which is widely used today in a large number of installations all over the world. Compared with traditional single baseline RTK technology, network RTK removes a significant amount of spatially correlated error due to the troposphere, ionosphere, and satellite orbit errors, and thus allows RTK positioning using reference station networks with inter-station distances of 40 kilometers or more while providing the performance of short baseline positioning.

Currently more than 2,500 reference stations are operating in networks in more than 30 countries using Trimble's GPSNet version of network RTK. Data processing in GPSNet uses the mathematically optimal Kalman filter technique to process data from all network reference stations. This approach models all relevant error sources, including satellite orbit and clock errors, reference station receiver clock errors, multipath, and particularly ionospheric and tropospheric effects.

To optimize real-time computational performance, our FAMCAR (Factorized Multi-Carrier Ambiguity Resolution) methodology is used to factorize uncorrelated error components into a bank of smaller filters, specifically a geometry filter, geometry-free filters, and code-carrier filters. This approach results in significantly higher computational efficiency. However, due to the fact that the geometry filter still contains a large number of states (several hundreds to a thousand or more states depending on the number of stations in the network), GPSNet until recently was able to process only 50 reference stations on a single PC server; larger networks were divided into sub-networks and operated by



INNOVATION INSIGHTS
with Richard Langley

As a network grows, more processing is required to generate corrections.

TABLE 1 Number of states in the centralized geometry filter

Stations	Satellites	States
20	12	328
	15	400
	18	472
40	12	608
	15	740
	18	872
80	12	1168
	15	1420
	18	1672
120	12	1728
	15	2100
	18	2472

multi-server solutions.

In recent years, more and more service providers have set up reference networks to provide nation-wide or region-wide RTK services. Many of them contain more than 50 reference stations; for example, Jenoba Corp., Japan (338 stations); E.ON Ruhrgas AG's ASCOS, Germany (more than 180 stations); Ordnance Survey, United Kingdom (86 stations); and many existing network operators intend to extend their networks to serve larger areas. Furthermore, with more signals from more satellites thanks to GNSS modernization efforts, even greater demands will be placed on the capabilities of network operators. In order to allow the processing of larger networks on one single PC, an efficient approach — the federated geometry filter — has been developed and implemented in Trimble's latest infrastructure software (GPSNet version 2.5).

Geometry Filter

The geometry filter plays an important role in the GNSS network data processing. It provides not only the float estimation of ionosphere-free ambiguities for later network ambiguity fixing, but also provides total zenith tropospheric propagation delay.

Centralized Filter. This filter usually runs as a centralized Kalman filter. The typical state vector in the filter consists of

- tropospheric zenith total delay (ZTD) per station
- receiver clock error per station
- satellite clock error per satellite
- ionosphere-free ambiguity per station per satellite
- orbit errors

TABLE 1 shows the number of states in the filter for a given number of stations and satellites observed at each station. For example, for a 20-station network with 12 satellites observed at each station, the filter has 328 states; for a 120-station network and 18 satellites observed at each station, the filter has 2,472 states. With the increase in the number of stations in the network and number of satellites observed at each station, the number of states and therefore processing time will increase dramatically.

FIGURE 1 shows the number of multiplications required for one filter step (one epoch of data sent through the filter) for a given number of stations with the assumption that 12 satellites are observed at each station. As the most time-consuming operation in the filter is the multiplication, this figure can be approximately interpreted

as the relationship between the number of stations and the computational load of the filter. In **Figure 1**, the blue bars give the number of multiplications in billions for numbers of station from 10 up to 120. The purple line in the figure represents the function $(37x)^3$, where x is the number of stations, which fits perfectly to the required multiplications. So, it is clear that the computational time increases cubically with the number of stations in the network.

Federated Filter. The federated Kalman filter was introduced by Neal Carlson in the late 1980s (see Further Reading). The basic idea of the federated filter is

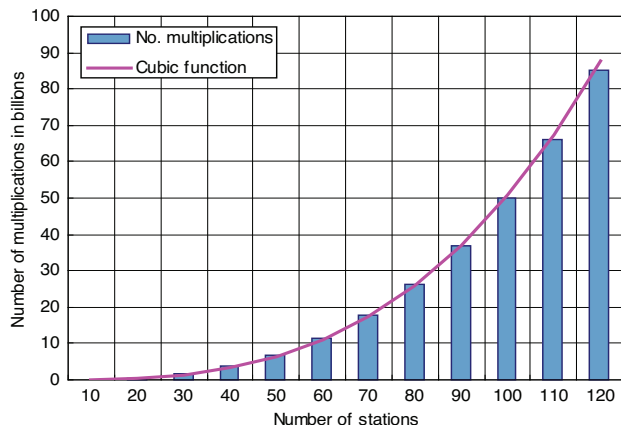
- A bank of local Kalman filters runs in parallel. Each filter operates on measurements from one local sensor only. Each filter contains unique states for one local sensor and common system states for all local sensors.

- A central fusion processor computes an optimally weighted least-squares estimate of the common system states and their covariance.

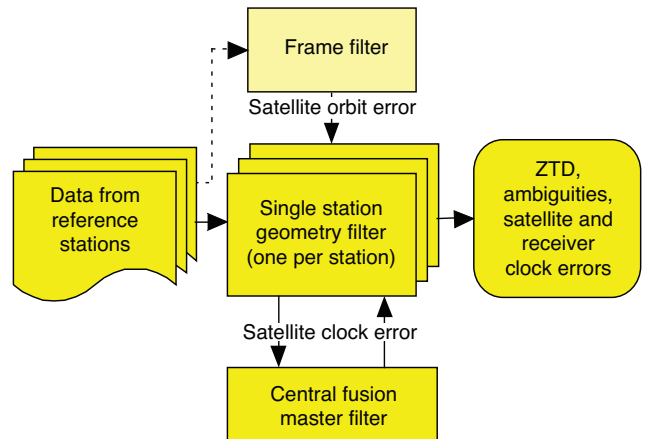
- Then, the result of the central fusion processor is fed back to each local filter to compute better estimates for the local unique states.

The main benefit of this approach is that each local filter runs with a reduced number of states and the computation time for the whole system increases only linearly with the increase in the number of local sensors. This significantly reduces the computational load compared to the centralized filter approach.

For GNSS network processing, each reference station can be treated as a local sen-



▲ FIGURE 1 Relation between number of reference stations and required multiplications in one filter step



▲ FIGURE 2 Block diagram of the federated geometry filter

sor with unique states like ZTD, receiver clock error, and ionosphere-free ambiguities ($2 + n$ states, where n is number of satellites in the system), and common states like satellite clock errors and orbit errors ($n + m \times n$ states, where n is number of satellites in the system and m is number of orbit-error parameters per satellite). Therefore the federated filter approach can be applied. As there are still too many common states, an additional step can be taken to further reduce the computational load. The satellite orbit error states are estimated with a frame filter. This frame filter uses only a subset of the reference stations in the network to estimate the orbit error parameters. Then the estimated orbit errors are applied directly to observations processed in the local filters.

FIGURE 2 illustrates the block diagram of the federated geometry filter for GNSS network processing. This approach contains one frame filter, a bank of single-station geometry filters (one per reference station), and one central fusion master filter.

Performance Analysis. Our performance analysis is divided into two parts. One is the post-processing performance comparison between the centralized geometry-filter approach and the federated geometry-filter approach. It focuses on the server performance - availability and reliability of the network processing and processing time. The other part is the real-time performance analysis focusing on the RTK rover positioning and ambiguity-fixing performance in the network.

Post-processing Performance. The post-processing performance study uses a post-processing version of GPSNet. The first test performed is to check the availability (percentage of fixed ambiguities) and reliability (percentage of correctly fixed ambiguities) with both the centralized geometry-filter approach and the federated

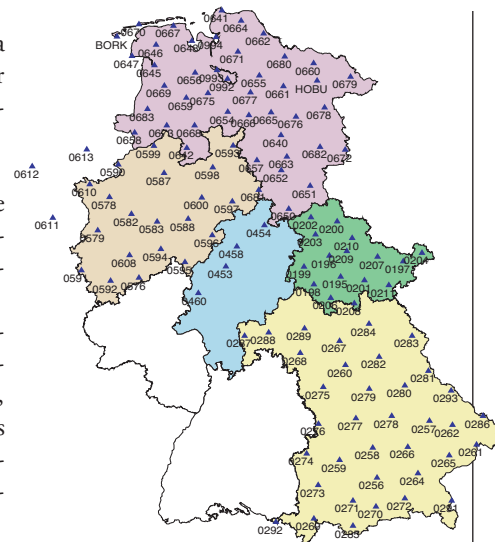
geometry-filter approach. Four days of data (days 289, 290, 291, and 322 of the year 2003) from the Bavarian Land Survey Department BLVG network (45 GPS stations, Germany) were used in the test.

TABLE 2 summarizes the test results. For the GPS-only network (BLVG), both approaches give similar results in terms of availability and reliability.

The second analysis is to check the processing time needed by the centralized and federated geometry-filter approaches. In this test, one day of data from 123 reference stations from five German states (Bavaria, Nordrhein-Westfalen, Hessen, Thuringen, and Niedersachsen) was used as shown in **FIGURE 3**.

From these 123 stations, we selected from 50 to 100 stations, in increments of 10 stations, to run network processing with both approaches. The total processing time (including data preparation, ionosphere modeling, and network ambiguity fixing) of each process for one day of data is summarized in **TABLE 3**. For a 50-station network, the federated filter approach takes 20 minutes to process the data, whereas the centralized filter takes 173 minutes. For a 100-station network, the federated filter approach takes 57 minutes, whereas the centralized filter approach takes 3581 minutes (nearly 2.5 days) to process one day of data, which means it is impossible to process data in real time. Table 3 also gives the ratio of processing time between the centralized filter and federated filter approaches. For a 50-station network, the federated filter approach is 8 times faster and for a 100-station network, the federated filter approach is 63 times faster than the centralized filter approach. This test proves that the federated filter approach is highly computationally efficient for large networks.

Real-Time Performance. For the real-time test, two GPSNet systems were set up



▲ FIGURE 3 Test network in Germany

in parallel. One ran the centralized filter approach. Real-time data streams from 45 stations in the BLVG network were used in this configuration. Another system ran the federated filter approach. Real-time data streams from more than 100 stations in the SAPOS network (the Satellite Positioning Service of the German State Survey) were used in this configuration. Two rover receivers located in the Trimble Terrasat office were used to verify the rover positioning and ambiguity-fixing performance. One of the VRS data streams generated from these two systems was streamed to each rover. The nearest reference station was 16 kilometers away in both cases.

TABLE 4 summarizes the statistics of position errors over one day, which indicate that the positioning performances from both systems are the same from a statistical point of view.

Another test conducted in real time is the check of RTK ambiguity-fixing performance. The test setup is the same as the positioning performance test. **TABLE 5** summarizes the RTK fixing performance during one day in terms of mean fixing time, the 68th, 90th, and 95th percentiles, and the minimum and maximum fixing times. Though the minimum and maximum fixing times for the rover in the system running the federated filter approach are longer than the centralized filter approach, other statistics are very much the same.

TABLE 2 Post-processing performance test (availability and reliability) in percent

NETWORK	Centralized Approach		Federated Approach	
	Availability	Reliability	Availability	Reliability
BLVG289	98.86	100	99.05	100
BLVG290	99.05	100	99.06	100
BLVG291	98.99	100	98.98	100
BLVG322	97.79	100	97.40	100

TABLE 3 Processing time comparison

Number of Stations	Centralized (minutes)	Federated (minutes)	Ratio
50	173.35	20.57	8.4
60	280.83	25.56	11.0
70	455.03	31.28	14.5
80	697.83	38.23	18.2
90	1152.47	53.15	21.7
100	3581.46	56.85	63.0

TABLE 4 Position error statistics

		Centralized (meters)	Federated (meters)
Mean	North	0.001	0.002
	East	-0.006	-0.006
	Height	0.001	0.005
1-Sigma	North	0.008	0.007
	East	0.005	0.005
	Height	0.013	0.013
RMS	North	0.007	0.007
	East	0.008	0.008
	Height	0.013	0.013

Improving Rover Performance

Latest developments have shown that it is possible to improve the rover positioning performance by using statistical information for the predicted residual error at the rover location. The models used in network RTK (such as the ionospheric, tropospheric, and orbit errors) reduce the magnitude of the error sources dramatically but they are unable to eliminate the errors completely. The predicted variance of the geometric and ionospheric corrections for each rover location can be computed from the available data for each satellite individually. These predicted values can be used in the rover to derive an optimum position solution using specific weighting mechanisms. The application of this approach is described below and results are presented showing the positioning performance due to the use of the computed statistical information.

The VRS method generates “optimized” corrections for individual rover locations. However, as mentioned, errors cannot be completely eliminated. Based on the available data, the density of the network, and

irregularities in atmospheric conditions, different residual errors will affect position solutions. Our VRS network server software is able to predict variances of residual errors at an individual rover location for each satellite in view. These parameters characterize the expected geometric and ionospheric errors at the rover. The stochastic parameters for the ionospheric error are given by

$$\sigma_i^2 = \sigma_{ic}^2 + \sigma_{id}^2 \times d^2$$

where σ_{ic} is the standard deviation accounting for constant dispersive prediction error, σ_{id} is the standard deviation for the distance-dependent dispersive prediction error, and d is the distance to the nearest physical reference station.

For the non-dispersive error, we use

$$\sigma_0^2 = \sigma_{oc}^2 + \sigma_{od}^2 \times d^2 + \sigma_{oh}^2 \times \Delta h^2$$

where σ_{oc} is the standard deviation accounting for constant non-dispersive prediction error, σ_{od} is the standard deviation for the distance-dependent non-dispersive prediction error, σ_{oh} is the standard deviation for the height-dependent non-dispersive prediction error, d is the distance to the nearest physical reference station, and Δh is the height difference to the reference station.

The distance-dependent part was introduced to describe the error growth with the distance to the nearest physical reference station. The height-dependent part is used to describe the error growth due to tropospheric delay. Typically the errors grow with distance from reference stations; that is, the estimates for the dispersive and non-dispersive errors at the rover location will be dependent on the

rover location in the network. As we can see in **FIGURE 4**, the error is small for some area around the reference stations and increases with distance. An alternative approach, which is desirable, is to continuously compute the error statistics in the network server software for the current rover position. In that case, the distance- and height-dependent parts of the equations describing the errors will be zero. Figure 4 shows typical error behavior for the ionospheric effect.

The stochastic parameters can be used in the rover to control the optimum weighting of VRS data for the individual satellites in the position solution and thus lead to increased position accuracy. This weighting approach can also be used to support the ambiguity search process and the optimum combination of L1 and L2 observations to derive a “minimum error” position estimate.

To verify this idea, we carried out tests with data from two different networks.

Terrasat Network. The first network is based on Terrasat-owned reference stations in the region surrounding Munich, Germany (see **FIGURE 5**).

The Hoehenkirchen station was not part of the network processing; it was used as a rover station only. The nearest reference station is Grosshoehenrain, which is 16 kilometers away. An optimum VRS data stream was generated for a full day and this data stream was used to position the Hoehenkirchen rover with the Trimble RTK engine. The RTK engine was run in the standard mode and in a modified mode, in which the RTK engine made use of the statistical information on ionospheric and geometric residual errors in the VRS data stream. In order to visualize the accuracy improvement, the full day was cut into 48 0.5-hour segments and the 3D root-mean-square (RMS) error for each 0.5-hour slot was computed and visualized. The green bars in **FIGURE 6** represent the RMS values for the standard procedure previously used in the RTK engine, whereas the red bars represent errors for the optimized solution. The cyan bars show the average predicted ionospheric errors. The graph shows that in almost all cases the optimized solution was able to reduce the position errors by up to a half. For some of the 0.5-hour slots, no

TABLE 5 RTK fixing performance in seconds

	Mean	68%	90%	95%	Min	Max
Centralized	25	27	30	34	13	508
Federated	25	27	29	35	16	561

improvement was obtained, which we will consider as a topic for further research. The problematic times are mainly the 0.5-hour periods with higher ionospheric residual errors than normal. This would be consistent with the ionosphere-free carrier-phase data providing the best solution here.

To show the individual errors in detail, a 0.5-hour period was selected and **FIGURES 7-9** show the errors for the standard solution in blue and the optimized solution in red in the north, east, and height components. It can be easily seen that the optimized solution provides much better accuracy in all three components.

Land Survey Network. The second network uses stations of the Bavarian Land Survey Department network (mainly non-Trimble receivers) and a rover location at the Terrasat office in Hoehenkirchen. Results were similar to those from the first test.

All our tests so far have shown that the use of the error estimates from the network have been able to improve the positioning accuracy considerably. The analysis we have done until now is a pure offline post-processing one, which allowed us to verify the usefulness of the approach.

The Radio Technical Commission for Maritime Services (RTCM) Special Committee 104 is discussing the potential creation of RTCM SC-104 Differential GNSS Service Standards version 3 messages to transmit these parameters from the network server to the user in the field for GPS and GLONASS satellites. These new messages will allow us to improve RTK accuracy in future systems.

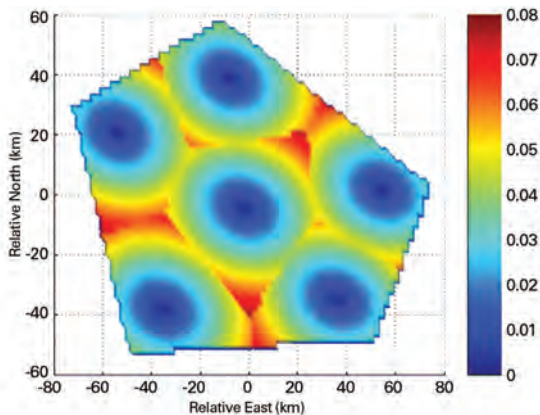
Initialization Performance. In addition to the RTK positioning accuracy, the RTK initialization performance can also be improved. First analysis of the “time to fix” per-

formance for the VRS networks we have analyzed show that the initialization time to fix all ambiguities can be reduced by a factor of approximately 30 percent compared to the already excellent ambiguity resolution performance typically seen in networked RTK.

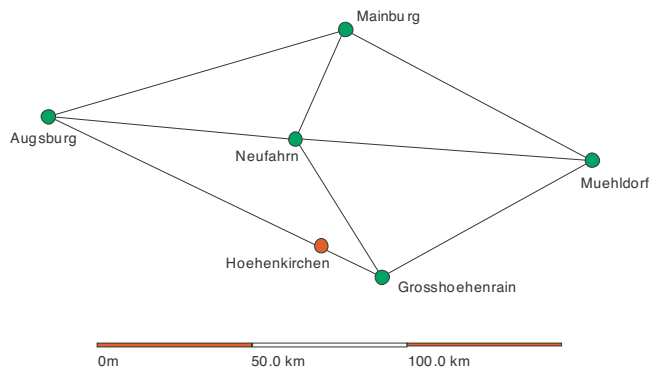
Summary

Continuing research and development of VRS technology allows us to provide solutions, which can process larger networks with more satellites and signals and support multiple satellite systems. Performance analyses for the federated filter approach show that availability and reliability of network processing are comparable and the rover performance stays the same compared to the centralized filter approach.

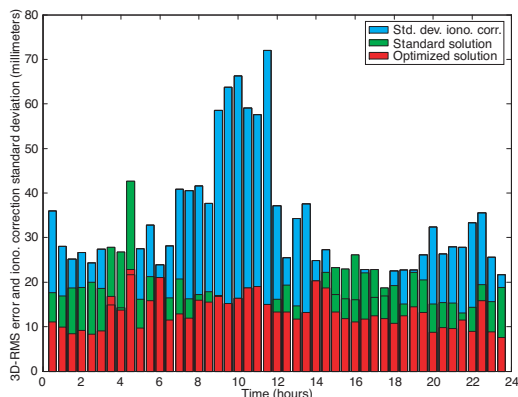
Using predicted dispersive and non-dispersive quality information computed from GPSNet for the rover location and all GPS



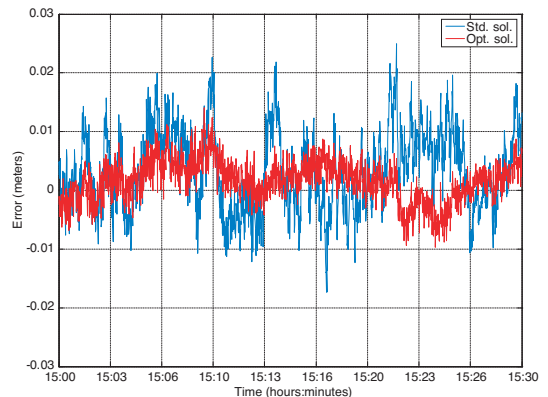
▲ **FIGURE 4** Typical ionospheric error distribution in a virtual reference station network during a period of strong ionospheric disturbance (values in meters)



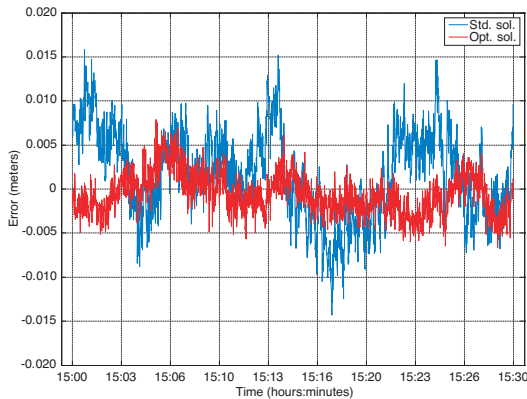
▲ **FIGURE 5** Terrasat reference station network in the vicinity of Munich



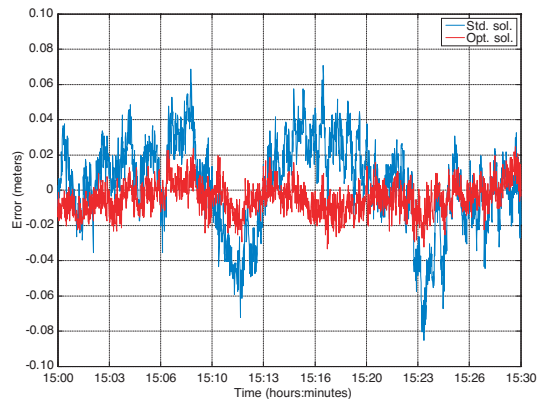
▲ **FIGURE 6** 3D-RMS values for 0.5-hour slots for the optimized solution in red, standard solution in green (ionosphere correction sigmas in cyan)



▲ **FIGURE 7** Terrasat network position errors in the north direction for the optimized solution in red (5 millimeters RMS) and the standard solution in blue (9 millimeters RMS)



▲ **FIGURE 8** Terrasat network position errors in the east direction for the optimized solution in red (2 millimeters RMS) and the standard solution in blue (6 millimeters RMS)



▲ **FIGURE 9** Terrasat network position errors in the height direction for the optimized solution in red (13 millimeters RMS) and the standard solution in blue (21 millimeters RMS)

and GLONASS satellites improves the rover positioning performance considerably when using the VRS technology. We hope that this technology will be accepted soon throughout the industry and will be available in almost all existing VRS networks.

Acknowledgments

We thank the land survey departments of Bavaria, Hessen, Nordrhein-Westfalen, Niedersachsen, Baden-Wuerttemberg, Thuringen, and E.ON Ruhrgas AG for providing recorded data and real-time data streams from their networks during our tests and for allowing us to use the data in our research. This article is based on the paper “Latest Developments in Network RTK

Modeling to Support GNSS Modernization” presented at the 2007 National Technical Meeting of The Institute of Navigation, San Diego, California, January 22–24. 🌐

Manufacturers

The *Terrasat* reference station network consists of **Trimble Navigation** (www.trimble.com) NetRS and NetR5 receivers. The *Terrasat* office in Hoehenkirchen uses *Trimble 5700* and *R8 GNSS* receivers.

HERBERT LANDAU received a Ph.D. in satellite geodesy from the University of the Federal Armed Forces, Munich, Germany, in 1988. At Trimble, he is Managing Director of Trimble *Terrasat GmbH*, Germany, and Director of the Trimble GNSS Algorithms and Infrastructure Software Group.

XIAOMING CHEN is a senior engineer at Trimble *Terrasat* responsible for R&D in the area of network solutions. He holds a Ph.D. in geodesy from Wuhan Technical University of Surveying and Mapping, Wuhan, China.

ADRIAN KIPKA received a Ph.D. in satellite geodesy from the Technical University of Darmstadt in 2006. Adrian joined Trimble in May 2005 and is working in the field of network solutions and RTK.

ULRICH VOLLATH received a Ph.D. in computer science from the Munich University of Technology in 1993. At Trimble *Terrasat* — where he has worked on GPS algorithms for more than 13 years — he is responsible for the RTK development team.

FURTHER READING

■ Kalman Filtering

“The Kalman Filter: Navigation’s Integration Workhorse” by L.J. Levy in *GPS World*, Vol. 8, No. 9, September 1997, pp. 65–71.

Theory and Application of Kalman Filtering by G. Minkler and J. Minkler, Magellan Book Company, Palm Bay, Florida, 1993.

■ Federated Kalman Filter

“Federated Square Root Filter for Decentralized Parallel Processes” by N.A. Carlson in *IEEE Transactions on Aerospace and Electronic Systems*, Vol. AES-26, No. 3, May, 1990, pp. 517–525.

■ Introduction to RTK Positioning

“RTK GPS” by R.B. Langley in *GPS World*, Vol. 9, No. 9, September 1998, pp. 70–76.

■ Network RTK and Virtual Reference Stations

“Will GALILEO/Modernized GPS Obsolete Network RTK” by X. Chen, U. Vollath, H. Landau in *Proceedings of ENC-GNSS 2004, Rotterdam*, Netherlands, May 16–19, 2004.

“Virtual Reference Station Systems” by H. Landau, U. Vollath, and X. Chen in *Journal of Global Positioning Systems*, Vol. 1, No. 2, 2002, pp. 137–143.

“Efficient Precision Positioning: RTK Positioning with Multiple Reference Stations” by J. Raquet and G. Lachapelle in *GPS World*, Vol. 12, No. 4, April 2001, pp. 48–53.

“Multi-Base RTK Positioning using Virtual Reference Stations” by U. Vollath, A. Deking, H. Landau, C. Pagels, and B. Wagner in *Proceedings of ION GPS 2000*, the 13th International Technical Meeting of the Satellite Division of The Institute of Navigation, Salt Lake City, Utah, September 19–22, 2000, pp. 123–131.

■ Factorized Multi-Carrier Ambiguity Resolution

“FAMCAR Approach for Efficient Multi-Carrier Ambiguity Estimation” by U. Vollath and K. Sauer in *Proceedings of ENC-GNSS 2004*, Rotterdam, Netherlands, May 16–19, 2004.